

FEEDBACK PARTICLE FILTER WITH STOCHASTICALLY PERTURBED INNOVATION AND ITS APPLICATION TO DUAL ESTIMATION *

ANGWENYI DAVID[†]

Abstract. Particle filters have, in recent years, been found to perform well in highly nonlinear problems as well as in estimation of parameters. However, there is still the problem of particle degeneracy in particle filters which has led to the invention of, among others, feedback particle filters. In this paper, we introduce a stochastically perturbed feedback particle filter and show that it is exact. The novelty is in the fact that the innovation process is stochastically perturbed. Resampled sinkhorn particle filter is also introduced. We then compare their performance with that of other filters in simultaneous state and parameter estimation.

Key words. Filtering, dual estimation, expectation maximization.

AMS subject classifications. 93E11, 65C40, 65C05

1. Introduction. Most state-space models are characterized by, among other things, parameters—which can be constant or varying. By a parameter is comprehended and signified a measurable factor which defines a model and influences its operation. As the parameter changes, so does the model; expressed differently, a parameter is unique to a model it characterises. The choice of a certain model, therefore, is achieved by choosing the right parameters. It occurs more often than not—in hidden Markov models, for instance—that measurements are available but the underlying signal is not readily apparent. This forms an example where parameter estimation is paramount: measurements are used to learn the model parameters, which, in turn, are used to fit the model.

For the ensuing discussion, we modify the usual signal and measurement equations, to include parameters, now and henceforth signified by a d -dimensional vector, θ , thus

$$(1.1a) \quad \text{Signal: } dx_t = f(x_t, \theta)dt + g(x_t)d\beta_t; \quad t_0 \leq t,$$

$$(1.1b) \quad \text{Measurement: } dy_t = h(x_t, \theta)dt + R^{1/2}(t)d\eta_t; \quad t_0 \leq t,$$

where

Term	Name	Dimension
x_t	state vector	$n \times 1$
$f(x_t, t)$	drift function	$n \times 1$
$g(x_t, t)$	diffusion function	$n \times m$
$\{\beta_t, t > t_0\}$	Brownian motion process	$m \times 1$
y_t	output vector	$r \times 1$
$h(x_t, t)$	sensor function	$r \times 1$
$R(t)$	time-function matrix	$r \times r$
$\{\eta_t, t > t_0\}$	standard Brownian motion process	$r \times 1$

Parameter estimation problem concerns finding the optimal parameter so that the signal best fits the data [10, 23]. This is, classically, achieved by optimization procedure where a cost function is minimized [13]. The cost function mostly defines the discrepancy between the state and the measurements. Intuitively, parameter estimation can be seen as a procedure for seeking a parameter value that gives the least discrepancy between the state and the corresponding measurements (also known as the algebraic distance or the residual). The method of least squares has been extensively used to define an objective function. Given the increment in measurement, dy_t , of the state, x_t , at time t , the objective function, $\mathcal{J}(\theta)$, in the least squares sense, is given by

$$(1.2) \quad \mathcal{J}(\theta) = \int_{t_0}^t w_t \|dy_t - h(x_t, \theta)dt\|^2,$$

where w_t is the weighting function.

Most commonly used procedures in the framework of least-squares include: linear least-squares, orthogonal least-squares, gradient weighted least-squares, bias corrected renormalization. This paper, however, attends not to the study of least-squares approaches. Suffice it to only direct the interested reader to the article [33] for an elaborate explanation and application of least-squares methods in computer vision. Instead, we study parameter estimation by means of filtering. But before that, we mention a few merits and demerits of least-squares and other methods defined by algebraic distances.

*Submitted to the editors on November 8, 2022.

Funding: This work was funded by the DAAD and the Kenya National Research Fund (NRF)

[†]Masinde Muliro University of Science and Technology (dangwenyi@mmust.ac.ke).

The use of algebraic distances in defining a cost function is computationally efficient and closed-form solutions are possible. The end result, however, is not satisfactory. This is due, in one part, to the fact that the objective function is mostly not invariant with respect to Euclidean transformations, for example, translation. This limits the coordinates systems to be used. In the other part, outliers may not contribute to the parameters the same way as inliers [33]. Other more satisfactory parameter estimation methodologies are highly desired. We consider, in this paper, the use of Bayesian inference techniques.

Estimation of parameters by means of a filter can be achieved in a number of ways; one of them being the use of the filter evidence, or its near approximation, and selection criteria for parameters which give a reasonable estimate of the evidence. The second method involves updating the parameters and the state at the same time. This is known as dual estimation, which further subdivides into joint estimation and a dual filter. Joint estimation entails subjoining the vector of parameters to the state vector to form an extended state-space. The filter is then implemented and run forward in time with the hope of filter convergence to the optimal state and parameter values. A dual filter, on the other hand, involves implementing a filter for the state and that of parameters simultaneously. The filter provides a self-correcting mechanism which may lead to convergence of state and parameter estimates.

Feedback particle filters [29, 30, 28, 31, 27, 1, 25] arose from the problem of particle degeneracy in particle filters, where particles lose weight substantially leading to poor filter performance. Feedback particle filters have been found to perform well and research is ongoing on the convergence and long-time performance of these filters [8, 18]. Other works related to this include time-delayed feedback control [26, 32]; the distinction from feedback particle filters being that the time-delay feedback control allows for direct control of parameters while the later uses a feedback gain which involves solving an associated partial differential equation [7].

The contribution of this paper is as follows: a new feedback particle filter is introduced based on the stochastic perturbation of the innovation process. this filter is shown to be exact. The feedback mechanism is then formulated from the perspective of the Schrödinger problem. Sinkhorn algorithm is used to bridge the feedback mechanism hence solving, iteratively, the Schrödinger problem. This yields the Sinkhorn particle filter. We investigate the performance of this filter in dual estimation and make comparisons with the performance of other extant filters.

The balance of this paper is arranged as follows. We first introduce different filters in time-continuous framework. This is done in section 2. The second part, that is section 3, is devoted to dual estimation where extended state-space formulation and the dual filter mechanism are elaborated. Application of the foregoing ideas to estimating constant parameters forms the closing part of this paper. Experimental results are in section 4, the discussion of results are in section 5, and the conclusions follow in section 6.

2. Filters. In this section, we introduce the filters used in this study.

2.1. FPF with stochastically perturbed innovation. The feedback particle filter (FPF) [29, 30, 28, 31, 27, 1, 25] arose from the need to overcome the challenges that come with application of existing filters to nonlinear state-space models. Extended Kalman filters, although meant to exploit the optimal performance of the Kalman filters in nonlinear systems, are greatly hampered by the need to compute the Jacobians. This challenge is more prevalent in approximate second-order filters, what with the need to compute the Hessians besides. Moreover, the computational cost in the aforementioned filters is compounded by the need to integrate the equation for evolution of covariance. Whereas particle filters hold promise for overcoming the challenge faced in using approximate filters in nonlinear settings, they, too, have their own challenges. Particle filters are sequential sampling Monte Carlo methods with particle degeneracy mitigating resampling steps. Although they are easy to implement, they suffer from the so-called sample impoverishment owing to frequent resampling—which is why resampling is done when the effective sample size has deteriorated to a given threshold. Despite the improvisations tending to the improvement of particle filters, the particle filters retain a comparatively high error covariance.

The idea behind feedback particle filters is designing the posterior density of each particle so that it matches, optimally, the true posterior. As will be seen in the ensuing argument, if one begins by setting the prior density of each particle to be the same as the true prior density, FPF yields the same posterior density as the true posterior at all subsequent times. This matching of the posterior density of the particles with the true posterior is arrived at by minimizing a cost function. To the present time, the cost function used is the Kullback-Leibler divergence between the two posteriors. Minimization of the cost function, in the first variation, yields a Poisson equation, the solution of which results in an optimal control input. The FPF is characterized by a controlled innovation process and the gain. It turns out, and this will be apparent shortly, that the FPF gain is obtained by differentiating the optimal control input with respect to the particles.

Motivated by the two variants of Ensemble Kalman Bucy filter (EnKBF) based on the perturbation of the innovation process [12, 22, 6], we obtain a stochastically-perturbed-innovation variant of the feedback particle filter by replacing the deterministic perturbation term to the innovation with a stochastic term. The McKean-Vlasov stochastic differential equations for the proposed feedback particle filter, for the state-space

model (1.1a) and (1.1b), omitting the parameter term, consists of the equation of the mean-field process,

$$(2.1) \quad d\bar{x}_t = f(\bar{x}_t)dt + g(\bar{x}_t)d\bar{\beta}_t + K(\bar{x}_t) \circ (dy_t + R^{1/2}(t)d\bar{\eta}_t - h(\bar{x}_t)dt),$$

and the finite M system of equations for the evolution of interacting hypotheses of the state, $X_t := \{x_t^i\}_{i=1}^M$; that is,

$$(2.2) \quad dx_t^i = f(x_t^i)dt + g(x_t^i)d\beta_t^i + K(x_t^i) \circ (dy_t + R^{1/2}(t)d\eta_t^i - h(x_t^i)dt),$$

where $\bar{\beta}_t$ and $\{\beta_t^i\}_{i=1}^M$ are independent copies of β_t and $\bar{\eta}_t$ and $\{\eta_t^i\}_{i=1}^M$ are independent copies of η_t ; such that, for a given function $q(x)$,

$$\pi_t[q(x) | Y_t] = \bar{\pi}_t[q(x) | Y_t] \approx \frac{1}{M} \sum_{i=1}^M q(x_t^i),$$

where $\pi_t = \text{Law}(x_t)$ and $\bar{\pi}_t = \text{Law}(\bar{x}_t)$.

For notational convenience, we rewrite the *controlled Stratonovich SDE* (2.2) as

$$(2.3) \quad dx_t = f(x_t)dt + g(x_t)d\beta_t + K(x_t) \circ (dy_t + R^{1/2}(t)d\eta_t - h(x_t)dt),$$

where $K = \nabla\phi(x)$ is the gain and $\phi(x)$ satisfies the Poisson equation,

$$(2.4a) \quad \nabla \cdot (\pi_t(x | Y_t) \nabla\phi(x)) = -(h(x_t, t) - \hat{h})\pi_t(x | Y_t)R^{-1}(t),$$

$$(2.4b) \quad \int \phi(x_t)\pi_t(x | Y_t)dx = 0,$$

where $\pi_t(x | Y_t)$ is the conditional density of the particle, x_t^i , given measurements $Y_\tau = \{y_\tau : t_0 \leq \tau \leq t\}$. $\{\eta_t\}$ is an r -dimensional vector standard Brownian motion process.

Written in Itô form, (2.3) becomes

$$(2.5) \quad dx_t = f(x_t, t)dt + g(x_t, t)d\beta_t + 2q(x_t, t)dt + K(x_t, t)(dy_t + R^{1/2}(t)d\eta_t - h(x_t, t)dt),$$

where $q(x_t, t)$ is given by

$$(2.6) \quad q_j(x_t, t) = \frac{R}{2} \sum_{k=1}^n K_k(x, t) \frac{\partial K_j}{\partial x_k},$$

As in the FPF with a deterministically perturbed innovation, the equation of evolution of the filtering density $\pi(x_t | Y_t)$ in the FPF with stochastically perturbed innovation is given by the Fokker-Planck equation to the SDE, (2.5); that is,

$$(2.7) \quad d\pi_t = \mathcal{L}(\pi_t)dt - \nabla \cdot (\pi_t K)dy_t - \nabla \cdot (\pi_t U)dt + \sum_{k,l=1}^n \frac{\partial^2}{\partial x_k \partial x_l} (\pi_t (K R K^T)_{kl})dt,$$

where $K = \nabla\phi$ is the solution of

$$(2.8) \quad \nabla \cdot (\pi_t K) = -\pi_t (h - \hat{h}_t)R^{-1}(t)$$

and U is then defined by

$$(2.9) \quad U = -Kh + 2q.$$

2.1.1. Exactness of FPF with stochastically perturbed innovation.

THEOREM 2.1 (Exactness of FPF with stochastic innovation). *Let initial filter posterior, π_{t_0} , be equal to the true posterior $\pi_{t_0}^*$ at time t_0 . Then the filter governed by (2.3) is exact.*

Proof. We now show, that beginning with the filter posterior

$$(2.10) \quad \pi_{t_0}(x | Y_{t_0}) = \pi_{t_0}^*(x | Y_{t_0}),$$

where $\pi_{t_0}^*(x | Y_{t_0})$ is the true posterior at initial time, t_0 , the filter posterior matches the true posterior at all times, t ; for then we demonstrate that the filter defined by (2.3) is exact. It suffices to show that the equations of evolution of the true posterior and filter posterior are the same; that is, (2.7) and

$$(2.11) \quad d\pi_t^* = \mathcal{L}(\pi_t^*)dt + \pi_t^*(h - \hat{h}_t)^T R^{-1}(t)(dy_t - \hat{h}_t dt),$$

are the same.

Multiplying U in (2.9) with $-\pi_t$ yields

$$(2.12) \quad \begin{aligned} -\pi_t U &= -\pi_t K h + 2\pi_t q \\ &= -\pi_t K (h - \hat{h}_t) - \pi_t K \hat{h}_t + 2\pi_t q, \end{aligned}$$

where in the second equality we introduce $\pi_t K \hat{h}_t - \pi_t K \hat{h}_t$. From (2.8) we have

$$(2.13) \quad -\pi_t (h - \hat{h}_t) = R(t) \nabla \cdot (\pi_t K_k).$$

Substituting (2.13) in (2.12) gives

$$(2.14) \quad -\pi_t U = KR(t) \nabla \cdot (\pi_t K) - \pi_t K \hat{h}_t + 2\pi_t q.$$

Using

$$(2.15) \quad \nabla \cdot (\pi [KRK^T]) = \pi KR \nabla \cdot (K) + KR \nabla \cdot (\pi K).$$

in (2.14) and noting the expression of $q(x_t, t)$ in (2.6), we get

$$(2.16) \quad -\pi U = -\nabla \cdot (\pi [KRK^T]) + \pi K \hat{h}_t.$$

whereupon taking divergence on both sides of (2.16) yields

$$(2.17) \quad -\nabla \cdot (\pi U) = -\sum_{l,k=1}^n \frac{\partial^2}{\partial x_l \partial x_k} (\pi [KRK^T]_{lk}) + \nabla \cdot (\pi K \hat{h}_t).$$

Finally, we substitute (2.8) and (2.17) for

$$-\nabla \cdot (\pi_t U) + \sum_{l,k=1}^n \frac{\partial^2}{\partial x_l \partial x_k} (\pi [KRK^T]_{lk})$$

and $\nabla \cdot (\pi_t K)$ in (2.7) to obtain

$$(2.18) \quad d\pi_t = \mathcal{L}(\pi_t)dt + \pi_t (h - \hat{h}_t)^T R^{-1}(t) (dy_t - \hat{h}_t dt),$$

which proves exactness. \square

Remark 2.2 (The gain). The equation from which the gain is obtained is the same for both FPF with deterministically perturbed innovation and that with stochastically perturbed innovation.

2.2. Ensemble Transform Particle Filter. The ensemble transform particle filter (ETPF) [20, 22] is, as the FPF, characterised by a control law, in the sense of optimal transportation, which moves the particles to the convenient position in the state space, thus improving upon the performance of the filter. The notable distinction between ETPF and particle filters with resampling is that the resampling step is replaced with a linear transformation. The transformation seeks to establish an optimal coupling between the prior ensemble and the posterior ensemble.

Most precisely, the linear transport problem is as follows:

$$(2.19) \quad T^* = \arg \min_{T \in \mathcal{R}^{M \times M}} \sum_{i,j=1}^M t_{ij} \|x_{t_n}^i - x_{t_n}^j\|^2,$$

under the constraints

$$(2.20) \quad \sum_{i=1}^M t_{ij} = \frac{1}{M}, \quad \sum_{j=1}^M t_{ij} = w_{t_n}^i, \quad \text{and } t_{ij} > 0,$$

where $\{w_{t_n}^i\}_{i=1}^M$ are weights at time $t_n = n\delta t$ and t_{ij} represents the element in row i and column j of the $M \times M$ matrix T . The weights are propagated as follows:

$$(2.21) \quad dw_t = \frac{1}{R} w_t^i (h(x_t^i) - \hat{h}_t)^T (dy_t - \hat{h}_t dt),$$

where

$$\hat{h}_t = \frac{1}{M} \sum_{i=1}^M h(x_t^i).$$

To avoid negative weights, (2.21) is approximated by

$$(2.22) \quad w_{t_{n+1}}^i \approx w_{t_n}^i \exp\left(-\frac{1}{2R}(h(x_{t_n}^i))^T h(x_{t_n}^i) \delta t - (h(x_{t_n}^i))^T \delta y_{t_n}\right),$$

and initialized with

$$w_{t_0}^i = \frac{1}{M}.$$

For the ETPF, the importance weights of the prior samples $\{x^i\}_{i=1}^M$ are given by $W_1 = \{w_1^i\}_{i=1}^M$ and $W_2 = \{w_2^i = 1/M\}_{i=1}^M$. Moreover, $X_1 = X_2 = \{x^i\}_{i=1}^M$. The posterior samples are given by

$$(2.23) \quad \tilde{x}_{t_n}^j = \frac{1}{M} \sum_{i=1}^M x_{t_n}^i t_{ij}^*.$$

2.3. Feedback formulation based on the Schrödinger problem. The Schrödinger problem [24] arises in the context of boundary value problems involving stochastic differential equations. Filtering problem can be cast as a Schrödinger problem, by means of Bayes' rule, and in the space of probability measures [2, 21]. In the ensuing argument, we invoke the algorithms used in optimal transportation [19] to solve the Schrödinger problem, which solution provides the estimates of the filtering distribution.

DEFINITION 2.3. Schrödinger problem:— Find two functions $\hat{\phi}_{t_n}(x_{t_n})$ and $\phi_{t_{n+1}}(x_{t_{n+1}})$, satisfying the following equations

$$(2.24a) \quad \pi_{t_n}(x_{t_n} | Y_{t_n}) = \pi_{t_n}^\phi(x_{t_n} | Y_{t_n}) \hat{\phi}_{t_n}(x_{t_n}),$$

$$(2.24b) \quad \pi_{t_{n+1}}(x_{t_{n+1}} | Y_{t_{n+1}}) = \pi_{t_{n+1}}^\phi(x_{t_{n+1}} | Y_{t_{n+1}}) \phi_{t_{n+1}}(x_{t_{n+1}}),$$

$$(2.24c) \quad \pi_{t_{n+1}}^\phi(x_{t_{n+1}} | Y_{t_{n+1}}) = \int \pi_{t_{n+1}}(x_{t_{n+1}} | x_{t_n}) \pi_{t_n}^\phi(x_{t_n} | Y_{t_n}) dx_{t_n},$$

$$(2.24d) \quad \hat{\phi}_{t_n}(x_{t_n}) = \int \pi_{t_{n+1}}(x_{t_{n+1}} | x_{t_n}) \phi_{t_{n+1}}(x_{t_{n+1}}) dx_{t_{n+1}},$$

where $\pi_{t_n}(x_{t_n} | Y_{t_n})$ and $\pi_{t_{n+1}}(x_{t_{n+1}} | Y_{t_{n+1}})$ are the marginal filtering distributions at times t_n and t_{n+1} , respectively.

When solved, (2.24a)–(2.24d) yield transition density

$$(2.25) \quad \pi_{t_{n+1}}^\phi(x_{t_{n+1}} | x_{t_n}) := \frac{\phi_{t_{n+1}}(x_{t_{n+1}})}{\hat{\phi}_{t_n}(x_{t_n})} \pi_{t_{n+1}}(x_{t_{n+1}} | x_{t_n}),$$

such that

$$(2.26) \quad \pi_{t_{n+1}}(x_{t_{n+1}} | Y_{t_{n+1}}) := \int \pi_{t_{n+1}}^\phi(x_{t_{n+1}} | x_{t_n}) \pi_{t_n}(x_{t_n} | Y_{t_n}) dx_{t_n},$$

where $\pi_{t_{n+1}}^\phi(x_{t_{n+1}} | x_{t_n})$ can be intuitively understood to define a coupling between the probability density function at time t_n , $\pi_{t_n}(x_{t_n} | Y_{t_n})$, and the filtering density function at time t_{n+1} , $\pi_{t_{n+1}}(x_{t_{n+1}} | Y_{t_{n+1}})$.

How do these notions fit in to filtering? Recall that, in the discrete setting, Bayes' Theorem gives an expression of the filtering density, $\pi_{t_{n+1}}(x_{t_{n+1}} | Y_{t_{n+1}})$, at time t_{n+1} as

$$(2.27) \quad \pi_{t_{n+1}}(x_{t_{n+1}} | Y_{t_{n+1}}) = \frac{\pi_{t_{n+1}}(y_{t_{n+1}} | x_{t_{n+1}}) \pi_{t_{n+1}}(x_{t_{n+1}} | Y_{t_n})}{\int \pi_{t_{n+1}}(y_{t_{n+1}} | x_{t_{n+1}}) \pi_{t_{n+1}}(x_{t_{n+1}} | Y_{t_n}) dx_{t_n}},$$

where

$$(2.28) \quad \pi_{t_{n+1}}(x_{t_{n+1}} | Y_{t_n}) = \int \pi_{t_{n+1}}(x_{t_{n+1}} | x_{t_n}) \pi_{t_n}(x_{t_n} | Y_{t_n}) dx_{t_n}$$

is the prediction density at time t_{n+1} [23, 11]. It then becomes apparent that (2.26) and (2.27) are equivalent. Notice that the Schrödinger problem reduces to (2.26) where, beginning with the filtering distribution $\pi_{t_n}(x_{t_n} | Y_{t_n})$, we directly obtain the filtering distribution $\pi_{t_{n+1}}(x_{t_{n+1}} | Y_{t_{n+1}})$ at time t_{n+1} via the twisted transition density $\pi_{t_{n+1}}^\phi(x_{t_{n+1}} | x_{t_n})$.

We use empirical estimates of the densities to solve (2.24a)–(2.24d) governing the Schrödinger problem; that is, given an ensemble $\{x_{t_n}^i\}_{i=1}^M$ at time t_n , we obtain an estimate of the prediction density, (2.28), by

$$(2.29) \quad \pi_{t_{n+1}}(x_{t_{n+1}} | Y_{t_n}) = \frac{1}{M} \sum_{i=1}^M \pi_{t_{n+1}}(x_{t_{n+1}} | x_{t_n}^i).$$

The filtering density, (2.28), is then empirically estimated as follows:

$$(2.30) \quad \pi_{t_{n+1}}(x_{t_{n+1}} | Y_{t_{n+1}}) = \frac{\frac{1}{M} \sum_{i=1}^M \pi_{t_{n+1}}(y_{t_{n+1}} | x_{t_{n+1}}) \pi_{t_{n+1}}(x_{t_{n+1}} | x_{t_n}^i)}{\int \pi_{t_{n+1}}(y_{t_{n+1}} | x_{t_{n+1}}) \pi_{t_{n+1}}(x_{t_{n+1}} | Y_{t_n}) dx_{t_n}}.$$

To solve the Schrödinger problem, (2.24a)–(2.24d), we make the following proposition

$$(2.31a) \quad \pi_{t_n}^\phi(x_{t_n} | Y_{t_n}) = \frac{1}{M} \sum_{i=1}^M \alpha^i \delta(x_{t_n} - x_{t_n}^i),$$

$$(2.31b) \quad \hat{\phi}_{t_n}(x_{t_n}) = \frac{1}{M} \sum_{i=1}^M \frac{1}{\alpha^i},$$

where

$$(2.31c) \quad \frac{1}{M} \sum_{i=1}^M \alpha^i = 1.$$

Substituting (2.31a) and (2.31b) in to (2.24a)–(2.24d) yields,

$$(2.32a) \quad \pi_{t_n}(x_{t_n} | Y_{t_n}) = \frac{1}{M} \sum_{i=1}^M \delta(x_{t_n} - x_{t_n}^i),$$

$$(2.32b) \quad \pi_{t_{n+1}}^\phi(x_{t_{n+1}} | Y_{t_{n+1}}) = \frac{1}{M} \sum_{i=1}^M \alpha^i \pi_{t_{n+1}}(x_{t_{n+1}} | x_{t_n}^i),$$

$$(2.32c) \quad \phi_{t_{n+1}}(x_{t_{n+1}}) = \frac{N}{\int(N) dx_{t_n} \frac{1}{M} \sum_{i=1}^M \alpha^i \pi_{t_{n+1}}(x_{t_{n+1}} | x_{t_n}^i)},$$

where

$$N = \pi_{t_{n+1}}(y_{t_{n+1}} | x_{t_{n+1}}) \sum_{i=1}^M \pi_{t_{n+1}}(x_{t_{n+1}} | x_{t_n}^i).$$

Therefore, one sets $\hat{\phi}_{t_n}(x_{t_n}) = \frac{1}{M} \sum_{i=1}^M \frac{1}{\alpha^i}$ and defines $\phi_{t_{n+1}}(x_{t_{n+1}})$ by (2.32c) in order to solve the Schrödinger problem; for then, given a twisted prediction density

$$(2.33) \quad \begin{aligned} \pi_{t_{n+1}}^\phi(x_{t_{n+1}} | Y_{t_n}) &= \frac{1}{M} \sum_{i=1}^M \pi_{t_{n+1}}^\phi(x_{t_{n+1}} | x_{t_n}^i) \\ &= \frac{1}{M} \sum_{i=1}^M \frac{\phi_{t_{n+1}}(x_{t_{n+1}})}{\hat{\phi}_{t_n}(x_{t_n}^i)} \pi_{t_{n+1}}(x_{t_{n+1}} | x_{t_n}^i), \end{aligned}$$

by (2.25), the relationship between the prediction density, $\pi_{t_{n+1}}^\phi(x_{t_{n+1}} | Y_{t_n})$, and the twisted prediction density, $\pi_{t_{n+1}}^\phi(x_{t_{n+1}} | Y_{t_n})$, is

$$(2.34) \quad \frac{\pi_{t_{n+1}}(x_{t_{n+1}} | Y_{t_n})}{\pi_{t_{n+1}}^\phi(x_{t_{n+1}} | Y_{t_n})} = \frac{\frac{1}{M} \sum_{i=1}^M \pi_{t_{n+1}}(x_{t_{n+1}} | x_{t_n}^i)}{\frac{1}{M} \sum_{i=1}^M \frac{\phi_{t_{n+1}}(x_{t_{n+1}})}{\hat{\phi}_{t_n}(x_{t_n}^i)} \pi_{t_{n+1}}(x_{t_{n+1}} | x_{t_n}^i)};$$

from which, if we draw samples from the twisted distribution

$$(2.35) \quad x_{t_n}^i \sim \pi_{t_{n+1}}^\phi(x_{t_{n+1}} | x_{t_n}^i),$$

then we can approximate the prediction density, $\pi_{t_{n+1}}^\phi(x_{t_{n+1}} | Y_{t_n})$, by

$$(2.36a) \quad \pi_{t_{n+1}}^\phi(x_{t_{n+1}} | Y_{t_n}) \approx \frac{1}{M} w^i \delta(x_{t_n} - x_{t_{n+1}}),$$

where

$$(2.36b) \quad w^i = \frac{\pi_{t_{n+1}}(x_{t_{n+1}} | Y_{t_n})}{\pi_{t_{n+1}}^\phi(x_{t_{n+1}} | Y_{t_n})}.$$

Now, suppose that we have $L = kM$, where $k \in \mathbb{N}$, samples $\{x_{t_n}^j\}_{j=1}^L$ drawn from $\pi_{t_n}(x_{t_n} | Y_{t_n})$. We obtain a bi-stochastic matrix $Q \in \mathbb{R}^{L \times M}$, which approximates the Markov process defined by $\pi(x_{t_{n+1}} | x_{t_n})$. The Schrödinger problem, (2.24a)–(2.24d), can then be recast as follows: Find two non-negative vectors $u \in \mathbb{R}^L$ and $v \in \mathbb{R}^M$ so that,

$$(2.37) \quad P^* = \text{diag}(u)Q\text{diag}(v)^{-1},$$

given that P^* belong to a polytope

$$U := \left\{ P \in \mathbb{R}^{L \times M} : P \geq 0, \sum_{j=1}^L p_{ji} = p_1, \sum_{i=1}^M p_{ji} = p_0 \right\}.$$

P^* is also a solution to the optimization problem defined by minimizing the distance between all possible bi-stochastic matrices P and Q ; that is,

$$(2.38) \quad P^* = \arg \min_{P \in U} \text{KL}(P \| Q),$$

where KL is the Kullback Leibler divergence between $P \in U$ and Q ; that is,

$$(2.39) \quad \text{KL}(P \| Q) := \sum_{j,i=1}^{L,M} p_{ji} \log \frac{p_{ji}}{q_{ji}},$$

where p_{ji} and q_{ji} are the elements of, respectively, matrices P and Q in row j and column i .

Now the feedback particle filter in the Schrödinger formulation is as follows: we first obtain an M -sized ensemble of states $\{\bar{x}_{t_n}^i\}_{i=1}^M$ using a forecast distribution, $\pi_{t_n}(\bar{x}_{t_n}^i | Y_{t_n})$, with respect to which each particle evolves according to the weak form of the Fokker-Planck equation [2]; that is

$$(2.40) \quad \bar{x}_{t_n}^i = \bar{x}_{t_{n-1}}^i + f(\bar{x}_{t_{n-1}}^i) \delta t.$$

Secondly, $L = kM$ ensembles are obtained as follows:

$$(2.41) \quad x_{t_n}^j = \bar{x}_{t_n}^j + g(t_n) d\beta_{t_n}^j,$$

where $\{\bar{x}_{t_n}^j\}_{j=1}^L$ are obtained by replicating each particle $\bar{x}_{t_n}^i$ k times. The weights are obtained using

$$(2.42) \quad w_{t_n}^j = \exp\left(-\frac{1}{2\delta t}(-2\delta y_{t_n}^T h(x_{t_n}^j) \delta t + h^T(x_{t_n}^j) h(x_{t_n}^j) \delta t^2)\right) w_{t_{n-1}}^j.$$

This gives a particle weight system, $\{x_{t_n}^j, \tilde{w}_{t_n}^j\}_{j=1}^L$, where $\tilde{w}_{t_n}^j$ signifies the normalised $w_{t_n}^j$ —normalisation done according to

$$\tilde{w}_{t_n}^j = \frac{w_{t_n}^j}{\sum_{j=1}^L w_{t_n}^j}.$$

By $Q \in \mathbb{R}^{L \times M}$, we denote and understand a matrix whose elements are

$$(2.43) \quad q_{ji} = \exp\left(-\frac{1}{2g^2\delta t} \|x_{t_n}^j - \bar{x}_{t_n}^i\|^2\right).$$

Then we solve the Schrödinger problem defined by (2.38), from whence we obtain P^* . P^* can be obtained, iteratively, by means of the Sinkhorn scheme stipulated in the following algorithm, whose implementation details are stipulated in [9].

Algorithm 2.1 Sinkhorn iteration**Require:** p_0 and p_1 .**Ensure:** P .

- 1: Compute Q and set $P^0 = Q$
- 2: **while** $k > 1$ **do**
- 3: Compute: $u^{k+1} = \text{diag}(\sum_{m=1}^M P^k)^{-1} p_1$.
- 4: Compute: $v^{k+1} = \text{diag}(\sum_{m=1}^M p_0)^{-1} \sum_{l=1}^L (\text{diag}(u^{k+1}) P^k)^T$.
- 5: Compute: $P^{k+1} = \text{diag}(u^{k+1}) P^k \text{diag}(v^{k+1})^{-1}$.
- 6: **end while**

Algorithm 2.2 Sinkhorn particle filter**Require:** $x_{t_0}^i, w_{t_0}^i = 1/M \forall i \in \{1, 2, \dots, M\}, k$, and $\delta y_{[t_0, t_T]}$.**Ensure:** $\hat{x}_{[t_0, t_T]}$.

- 1: **for** $n = 1$ **to** $N, \delta t > 0$ **do**
- 2: **for** $i = 1$ **to** M **do**
- 3: Obtain $\bar{x}_{t_n}^i$ using (2.40)
- 4: **for** $j = 1$ **to** L **do**
- 5: Replicate $\bar{x}_{t_n}^i$ k times and obtain $x_{t_n}^j$ using (2.40)
- 6: Compute weights $w_{t_n}^j$ using (2.42)
- 7: Compute q_{ji} using (2.43)
- 8: **end for**
- 9: Calculate P^* by solving the the Schrödinger problem via [Algorithm 2.1](#)
- 10: Compute the filtered particles $\tilde{x}_{t_n}^i$ using (2.44)
- 11: **end for**
- 12: Compute $\hat{x}_{t_n} = \frac{1}{M} \sum_{i=1}^M \tilde{x}_{t_n}^i$
- 13: **end for**

Filtered particles are eventually obtained thus

$$(2.44) \quad \tilde{x}_{t_n}^i = \sum_{j=1}^L x_{t_n}^j p_{ji}^* + g(\delta t)^{1/2} \xi_{t_n}^i, \quad \xi_{t_n}^i \sim \mathcal{N}(\bar{0}_{n \times 1}, \mathbf{I}_{n \times n}),$$

where $\bar{0}_{n \times 1}$ and $\mathbf{I}_{n \times n}$ are, respectively, the null vector and the identity matrix of sizes as indicated in the subscripts. This yields the proposed Sinkhorn particle filter (SPF), whose summary is in [Algorithm 2.2](#).

Alternatively to obtaining the particles by means of (2.44), we can resample $\{x_{t_n}^j\}_{j=1}^L$ such that

$$(2.45) \quad \mathbb{P}(x_{t_n}^i = x_{t_n}^j) = p_{ji}^*, \quad \forall i = 1, 2, \dots, M.$$

This results in the resampling Sinkhorn Particle filter (RSPF), the summary of which is in [Algorithm 2.3](#).

Algorithm 2.3 Resampling Sinkhorn particle filter**Require:** $x_{t_0}^i, w_{t_0}^i = 1/M \forall i \in \{1, 2, \dots, M\}, k$, and $\delta y_{[t_0, t_T]}$.**Ensure:** $\hat{x}_{[t_0, t_T]}$.

- 1: **for** $n = 1$ **to** $N, \delta t > 0$ **do**
- 2: **for** $i = 1$ **to** M **do**
- 3: Obtain $\bar{x}_{t_n}^i$ using (2.40)
- 4: **for** $j = 1$ **to** L **do**
- 5: Replicate $\bar{x}_{t_n}^i$ k times and obtain $x_{t_n}^j$ using (2.40)
- 6: Compute weights $w_{t_n}^j$ using (2.42)
- 7: Compute q_{ji} using (2.43)
- 8: **end for**
- 9: Calculate P^* by solving the the Schrödinger problem via [Algorithm 2.1](#)
- 10: Resample the particles according to (2.45) to obtain the filtered particles $\tilde{x}_{t_n}^i$
- 11: **end for**
- 12: Compute $\hat{x}_{t_n} = \frac{1}{M} \sum_{i=1}^M \tilde{x}_{t_n}^i$
- 13: **end for**

3. Dual estimation. Dual estimation comprehends simultaneous estimation of state and parameters by means of an appropriate filter. The self-correcting mechanism of the filter is taken advantage of to converge to both the true state and the true parameters. Depending on the initial parameter, the filter sooner or later converges to the true parameter value. Dual estimation can be achieved in two ways: joint estimation and by a dual filter [3, 15, 14, 17, 4]. In this section, and the rest of this paper, we shall assume that the parameters are static; that is, time-invariant.

3.1. Joint estimation (augmented state-space). In joint estimation, the state vector is augmented with the vector of parameters to form an extended state-space and then the filter is run forward in time for an update of both the state and the parameters. The parameters are induced with artificial dynamics, or are made to assume a random walk; that is, respectively,

$$(3.1) \quad dz_t = \zeta_t; \quad t_0 \leq t,$$

where

$$(3.2a) \quad dz_t = \begin{pmatrix} dx_t \\ d\theta_t \end{pmatrix} \text{ and } \zeta_t = \begin{pmatrix} f(x_t, \theta)dt + g(x_t)d\beta_t \\ 0 \end{pmatrix},$$

or where

$$(3.2b) \quad \zeta_t = \begin{pmatrix} f(x_t, \theta)dt + g(x_t)d\beta_t \\ \sigma d\chi_t \end{pmatrix},$$

in which $\{\chi_t, t > t_0\}$ is a d -dimensional standard Brownian motion vector process and σ is a small constant. A filter is then implemented with the augmented state z_t in the place of x_t . The demerit of this method is that the extended state-space has an increased degree of freedom owing to many unknowns, of both the state and the parameters, which renders the filter unstable and intractable, especially in nonlinear models [16]. Joint estimation is also known as expectation maximisation [23].

3.2. Test example. We now consider a scalar example in order to test the performance of different filters under joint estimation of both the state and the parameters.

Example 3.1: Scalar SDE

Consider the following linear Gaussian Itô state space model.

$$(3.3a) \quad dx_t = (ax_t + b)dt + Q^{1/2}dv_t; \quad t_0 \leq t,$$

$$(3.3b) \quad dy_t = cx_tdt + R^{1/2}dw_t; \quad t_0 \leq t,$$

where $\{v_t\}$ and $\{w_t\}$ are standard Brownian motion processes with, respectively,

$$\mathbb{E}\{dv_tdv_t^T\} = dt \text{ and } \mathbb{E}\{dw_tdw_t^T\} = dt.$$

Let the state, x_t , at time t_0 be $x_{t_0} \sim \mathcal{N}(0, 0.001)$. Let, moreover, x_{t_0} , $\{v_t, t \geq t_0\}$ and $\{w_t, t \geq t_0\}$ be uncorrelated. We take $a = -0.2$, $b = 0.2$, $c = 1.01$, $Q = 0.001$, $R = 0.001$ and proceed to simultaneously estimate the state, x_t , and the parameters, a and b using different filters.

4. Experimental results. The following panels show the results obtained using EnKBF, BPF (bootstrap particle filter) [2, 5], FPF (feedback particle filter with kernel-based gain approximation), ETPF—ensemble transform particle filter [22] introduced in Subsection 2.2 and RSPF.

We now plot the box-plots, the better to see the distribution of parameter estimates in the results shown in Figure 1, beyond time 30.

	EnKBF	BPF	FPF	ETPF	RSPF
M	1000	1000	1000	100	1000
Time in seconds	21.69	11.78	233.66	334.78	732.12

TABLE 1

A table showing run-time and number of particles for results shown in Figure 2 for different filters. This is an output of 2.3 GHz Intel Core i5 processor.

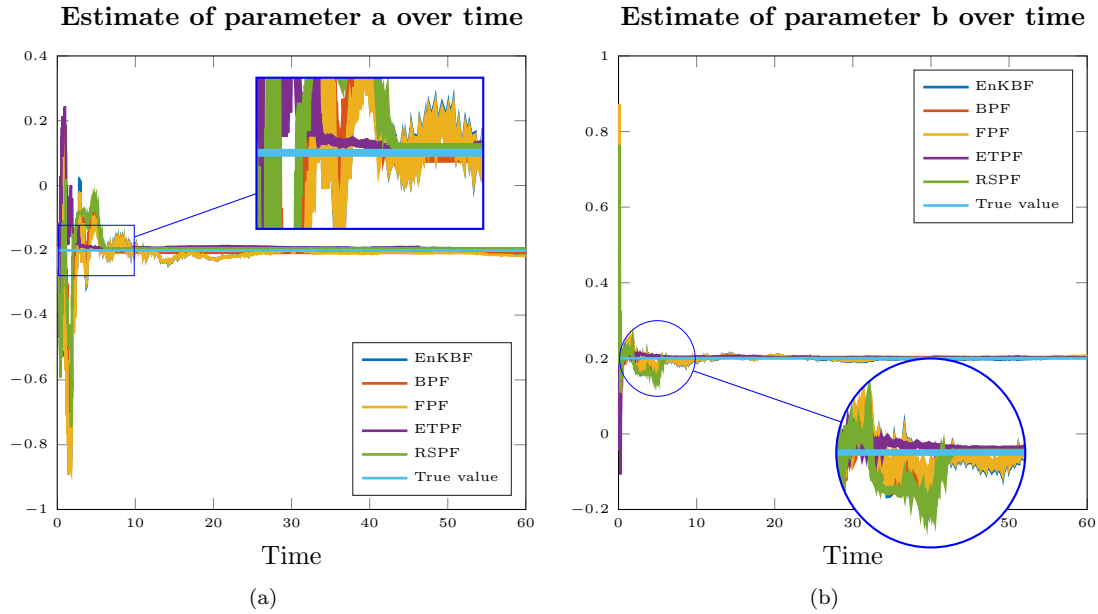


FIG. 1. Plots showing:- (a) estimates of parameter a and (b) estimates of parameter b over time using $EnKBF$, BPF , FPF , $ETPF$ and $RSPF$. The true parameter values are, respectively, $a = -0.2$ and $b = 0.2$. The plots indicate that all the filters converge to the true parameter values. The time step used is $\delta t = 0.02$.

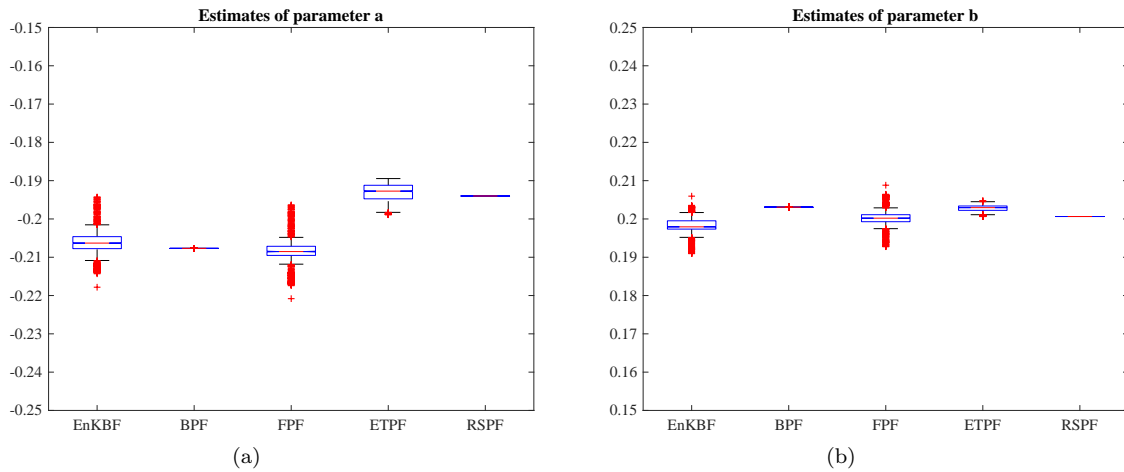


FIG. 2. Box-plots (a) and (b) showing, respectively, the distribution of estimates of parameters a and b obtained using $EnKBF$, BPF , FPF , $ETPF$ and $RSPF$. The gain in the FPF is computed using the kernel based gain approximation method [2]. In both cases, the $EnKBF$ and FPF register more dispersive results with more outliers than the BPF , $ETPF$ and $RSPF$.

5. Discussion of experimental results. The $EnKBF$, BPF , FPF , $ETPF$ and $RSPF$ yield converging results to the true parameter values but with some margin of error. From Figures 1(a) and 1(b), it is evident that the $ETPF$ yields a faster converging results compared to the other filters. Furthermore, the FPF takes more time before a steady value is obtained as compared to other filters.

From Table 1, the BPF is faster compared to other methods. FPF is slower whilst $ETPF$ is the slowest, seeing that the number of particles used is 100. The gain in the FPF is computed using the kernel based gain approximation method. The reason for this is that FPF involves a lengthy procedure for gain computation, at each iteration. On the other hand, The $ETPF$ involves frequent solution of optimal transport problem. In this example, earth movers distance (EMD) algorithms were used in the $ETPF$. As a remedy, faster optimal transport algorithms, for example the Sinkhorn iteration, can be viable [9]. Although the $RSPF$ takes much time, the result, as seen in Figure 2, is more accurate compared to that obtained from other methods. This is further shown in Figure 3, where the lowest RMSE is posted by $RSPF$ indicating that it is more accurate compared to the rest of the filters.

6. Conclusions. This paper has accomplished a number of purposes. In the first place, a variant of feedback particle filter has been introduced with stochastically perturbed innovation process and it has been shown that the proposed filter is exact; that is to say, the filter posterior maps the true posterior when the

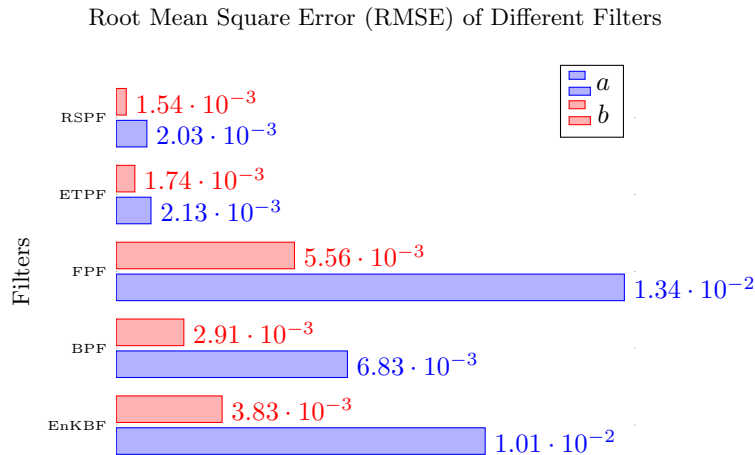


FIG. 3. Plot showing the RMSE in estimation of parameters a and b using EnKBF, BPF, FPF, ETPF and RSPF. ETPF and RSPF register a small RMSE which shows that they perform better than the rest of the filters. RSPF, however, although having the lowest RMSE, is run with 1000 ensembles while ETPF is run with 100 ensembles because of time constraints.

filter prior is set equal to the true prior. Sinkhorn particle filters have been introduced beginning with optimal transport notions as postulated by Schrödinger. Finally, Comparison of the performance of EnKBF, BPF, FPF, ETPF and RSPF filters in joint estimation of both the state and parameters has been carried out by means of a scalar example. From the results, ETPF seems to converge to the true parameter faster than the other filters. In as much as RSPF takes more time, the boxplots indicate that RSPF is more accurate compared to EnKBF, BPF, FPF, and ETPF. Moreover, the plot of RMSE indicates that RSPF is more accurate compared with the other filters.

Acknowledgments. I would like to acknowledge the assistance of Professor Dr. Sebastian Reich, of Potsdam University, Germany, in supervising my doctoral research [2], of which this paper is part.

REFERENCES

- [1] T. AMIRHOSSEIN, J. DE WILJES, G. PRASHANT, AND S. REICH, *Kalman Filter and its Modern Extensions for the Continuous-time Nonlinear Filtering Problem*, Psychological Review, (2016).
- [2] D. ANGWENYI, *Time-continuous state and parameter estimation with application to hyperbolic SPDEs*, doctoralthesis, Universität Potsdam, 2019, <https://doi.org/10.25932/publishup-43654>.
- [3] D. ANGWENYI, *Estimation of spatially varying parameters with application to hyperbolic SPDEs*, arXiv:2107.07246v1, (2021).
- [4] D. ANGWENYI, J. DE WILJES, AND S. REICH, *Interacting Particle Filters for Simultaneous State and Parameter Estimation*, arXiv: 1709.09199v1, (2017).
- [5] S. ARULAMPALAM, S. MASKELL, N. GORDON, AND T. CLAPP, *A Tutorial on Particle Filters for Online Nonlinear/Non-Gaussian Bayesian Tracking*, IEEE Transactions on Signal Processing, 50 (2002), pp. 174 – 188.
- [6] K. BERGEMANN AND S. REICH, *An Ensemble Kalman-Bucy Filter for Continuous Data Assimilation*, Meteorolog. Zeitschrift, 21 (2012), pp. 213 – 219.
- [7] K. BERNTORP, *Feedback particle filter: Application and evaluation.*, in 2015 18th International Conference on Information Fusion, 2015, pp. 1633–1640.
- [8] X. CHEN, X. LUO, J. SHI, AND S. YAU, *General convergence result for continuous-discrete feedback particle filter.*, International Journal of Control, (2021).
- [9] M. CUTURI, *Sinkhorn Distances: Lightspeed Computation of Optimal Transportation Distances*, arXiv:1306.0895v1 [stat.ML], (2013).
- [10] G. A. EINICKE, *Smoothing, Filtering and Prediction: Estimating the Past, Present and Future*, InTech, Janeza Trdine 9, 51000 Rijeka, Croatia, 2012.
- [11] A. JAZWINSKI, *Stochastic Processes and Filtering Theory*, Academic Press, New York, 1970.
- [12] K. LAW, A. STUART, AND K. ZYGALAKIS, *Data Assimilation: A Mathematical Introduction*, Springer, 2015.
- [13] J. LEWIS, S. LAKSHMIVARAHAN, AND S. DHALL, *Dynamic Data Assimilation: A Least Squares Approach*, Cambridge University Press, 2006.
- [14] J. W. C. V. LINT, S. P. HOOGENDOORN, AND A. HAGYI, *Dual EKF State and Parameter Estimation in Multi-Class First-order Traffic Models*, in Proceedings of the 17th World Congress, The International Federation of Automatic Control, Seoul, Korea, July 6-11 2008.
- [15] H. LÜ, Z. YU, Y. ZHU, S. DRAKE, Z. HAO, AND E. A. SUDICKY, *Dual State-Parameter Estimation of Root Zone Soil Moisture by Optimal Parameter Estimation and Extended Kalman Filter Data Assimilation*, Advances in Water Resources, 34 (2011), pp. 395–406.
- [16] H. MORADKHANI, S. SOROOSHIAN, H. GUPTA, AND P. HOUSER, *Dual State-Parameter Estimation of Hydrological Models Using Ensemble Kalman Filter*, Advances in Water Resources, 28 (2005), pp. 135–147. Elsevier.
- [17] H. MORADKHANI, S. SOROOSHIAN, H. V. GUPTA, AND P. R. HOUSER, *Dual State-Parameter Estimation of Hydrological Models Using Ensemble Kalman Filter*, Advances in Water Resources, 28 (2005), pp. 135–147.
- [18] S. PATHIRAJA AND W. STANNAT, *Analysis of the feedback particle filter with diffusion map based approximation of the gain.*,

- Foundations of Data Science, 3 (2021).
- [19] G. PEYRÉ AND M. CUTURI, *Computational Optimal Transport*, arXiv: 1803.00567v1 [stat.ML], 2018.
 - [20] S. REICH, *A Nonparametric Ensemble Transform Method for Bayesian Inference*, SIAM Journal of Scientific Computing, 35 (2013), pp. A2013–A2024.
 - [21] S. REICH, *Data assimilation: The Schrödinger perspective*, Acta Numerica, 28 (2019), p. 635–711, <https://doi.org/10.1017/S0962492919000011>.
 - [22] S. REICH AND C. COTTER, *Probabilistic Forecasting and Bayesian Data Assimilation*, Cambridge University Press, 2015.
 - [23] S. SÄRKKÄ, *Bayesian Filtering and Smoothing*, Cambridge University Press, Cambridge, 2013.
 - [24] E. SCHRÖDINGER, *Über die Umkehrung der Naturgesetze*, Sitzungsberichte der Preußischen Akademie der Wissenschaften, Physikalisch-mathematische Klasse, (1931), pp. 144–153.
 - [25] A. TAGHVAEI AND P. G. MEHTA, *Error analysis of the stochastic linear feedback particle filter*, arXiv: 1809.07892v1, (2018).
 - [26] E. XU, Y. ZHANG, AND Y. CHEN, *Time-delayed local feedback control for a chaotic finance system.*, Journal of Inequalities and Applications, (2021).
 - [27] T. YANG, *Feedback Particle Filter and its Applications*, PhD thesis, Department of Mechanical Science and Engineering, University of Illinois at Urbana-Champaign, 2014.
 - [28] T. YANG, R. LAUGESSEN, P. MEHTA, AND S. MEYN, *Multivariable feedback particle filter*, in Proceedings of the 51st IEEE Conference on Decision Control, 2012, pp. 4063–4070. Maui, HI.
 - [29] T. YANG, P. MEHTA, AND S. MEYN, *A Mean-field Control-oriented Approach to Particle Filtering*, in Proceedings of American Control Conference, 2011, pp. 2037–2043.
 - [30] T. YANG, P. MEHTA, AND S. MEYN, *Feedback Particle Filter with Mean-field Coupling*, in Proceedings of IEEE 50th Conference on Decision and Control, 2011, pp. 7909–7916. Orlando, FL.
 - [31] T. YANG, P. MEHTA, AND S. MEYN, *Feedback Particle Filter*, IEEE Transactions in Automatic Control, 58 (2013), pp. 2465–2480.
 - [32] A. ZACHAROVA, N. SEMENOVA, V. ANISHCHENKO, AND E. SCHOELL, *Time-delayed feedback control of coherence resonance chimeras.*, An Interdisciplinary Journal of Nonlinear Science., 27 (2017).
 - [33] Z. ZHANG, *Parameter Estimation Techniques: A Tutorial with Applications to Conic Fitting*, Image and Vision Computing, (1997). Elsevier.